Published in final edited form as:
Cell. 2013 June 6; 153(6): 1252–1265. doi:10.1016/j.cell.2013.04.056.

Regulation of Axon Guidance by Compartmentalized Nonsense-Mediated mRNA Decay

Dilek Colak[1], **Sheng-Jian Ji**[1], **Bo T. Porse**[2,3,4], and **Samie R. Jaffrey**[1]

[1]Department of Pharmacology, Weill Medical College, Cornell University, New York, NY 10065, USA

[2]The Finsen Laboratory, Rigshospitalet, Faculty of Health Sciences, University of Copenhagen, Copenhagen 2200, Denmark

[3]Biotech Research and Innovation Center (BRIC), University of Copenhagen, Copenhagen 2200, Denmark

[4]Danish Stem Cell Centre (DanStem) Faculty of Health Sciences, University of Copenhagen, Copenhagen 2200, Denmark

Abstract

SUMMARY—Growth cones enable axons to navigate towards their targets by responding to extracellular signaling molecules. Growth cone responses are mediated in part by the local translation of axonal mRNAs. However, the mechanisms that regulate local translation are poorly understood. Here we show that Robo3.2, a receptor for the Slit family of guidance cues, is synthesized locally within axons of commissural neurons. *Robo3.2* translation is induced by floor plate-derived signals as axons cross the spinal cord midline. *Robo3.2* is also a predicted target of the nonsense-mediated mRNA decay (NMD) pathway. We find that NMD regulates Robo3.2 synthesis by inducing the degradation of *Robo3.2* transcripts in axons that encounter the floor plate. Commissural neurons deficient in NMD proteins exhibit aberrant axonal trajectories after crossing the midline, consistent with misregulation of Robo3.2 expression. These data show that local translation is regulated by mRNA stability, and that NMD acts locally to influence axonal pathfinding.

INTRODUCTION

NMD is a mechanism that regulates protein expression by controlling the stability of specific transcripts (Doma and Parker, 2007; Hodgkin et al., 1989; Leeds et al., 1992). NMD was initially identified as a pathway that degrades transcripts containing mutations or DNA rearrangements that result in a premature stop codon (Lejeune and Maquat, 2005; Li and Wilkinson, 1998; Maquat et al., 1981). NMD is triggered when a ribosome at the stop codon detects downstream mRNA-bound proteins that participate in splicing reactions. After splicing reactions, a complex of proteins involved in splicing remain bound at the junction between each exon. In most transcripts, all exon junction complexes are upstream of the stop codon and are removed during the initial rounds of translation (Chang et al., 2007; Dostie

Correspondence should be addressed to S.R.J. (srj2003@med.cornell.edu)..

and Dreyfuss, 2002; Ishigaki et al., 2001). However, in the case of mutations that result in a new stop codon, some exon junction complexes might be present downstream of the stop codon. This initiates a process that ultimately leads to mRNA degradation (Carter et al., 1995; Zhang et al., 1998).

Recent findings have suggested that NMD may have broader roles in regulating mRNA and protein expression. In some cases, endogenously expressed transcripts appear to be NMD targets due to introns in the 3′-untranslated region or alternative splicing events that result in a stop codon that is followed by an exon junction complex (Giorgi et al., 2007; McGlincy and Smith, 2008; Weischenfeldt et al., 2012; Zheng et al., 2012). NMD appears to regulate the stability of both of these types of transcripts, thereby affecting the levels of the translated protein. However, the extent to which the NMD-dependent degradation of these transcripts is physiologically relevant is not clear.

An example of a transcript that has important physiological roles and is also a predicted NMD target is *Robo3.2* (Black and Zipursky, 2008). The *Robo3.2* isoform differs from *Robo3.1* by the presence of a retained intron resulting in a new stop codon that is upstream of an exon junction complex. As a result, *Robo3.2* is a predicted NMD target.

During commissural axon guidance in the spinal cord, axons are initially attracted to, and upon crossing, become repulsed from the ventral midline. These sequential events are governed by guidance cues released from the floor plate, which is a region of specialized glial cells in the midline (Long et al., 2004; O'Donnell et al., 2009; Serafini et al., 1994). The precise regulation of the spatiotemporal expression of Robo3.1 and Robo3.2, which are alternatively spliced forms of *Robo3,* is critical for the proper guidance of commissural axons (Chen et al., 2008). As the axons grow towards the midline, they express Robo3.1 but not Robo3.2, although the *Robo3.2* transcript is abundant in commissural neurons (Chen et al., 2008). However, after the commissural axons have crossed through the midline, Robo3.2 protein is induced and selectively detected in the postcrossing axonal segment and Robo3.1 protein is downregulated (Chen et al., 2008). Robo3.1 allows axons to approach the midline by suppressing the activity of Robo1 and Robo2, which otherwise mediate repulsion from the midline. Following midline crossing, axons are repelled from the midline due to the loss of Robo3.1 and the expression of Robo3.2, which supports the activity of Robo1 and Robo2 (Chen et al., 2008). The mechanism that controls the compartmentalized expression of Robo3.2 is not known.

Recent studies have identified local translation as a mechanism that controls growth cone responses to axon guidance cues (Campbell and Holt, 2001; Jung et al., 2012; Leung et al., 2006). During embryonic development, a small subset of cellular mRNAs is trafficked into axons and locally translated (Campbell and Holt, 2001; Jung et al., 2012; Tennyson, 1970). Local translation affects the protein composition of growth cones, thereby affecting the responses to guidance cues. The mechanisms that regulate the expression levels of specific axonal transcripts are not fully understood.

Here we show that axon guidance is physiologically regulated by NMD. We show that the *Robo3.2* transcript is selectively trafficked to commissural axons, and is translated when axons are exposed to floor plate signals in the spinal cord midline. Upon translation, *Robo3.2* transcripts are targeted by NMD, ultimately limiting Robo3.2 protein levels in postcrossing axons. Selective deletion of the essential NMD component *Upf2* from commissural neurons results in elevated levels of Robo3.2 protein in axons and aberrant postcrossing axonal trajectories in embryonic spinal cord. Additionally, we find that proteins that mediate NMD are highly enriched in growth cones from diverse neuronal types. These

data demonstrate a role for NMD in influencing local translation pathways that regulate axon guidance and potentially other growth cone functions.

RESULTS

Robo3.2 Protein Is Induced by Floor Plate-Derived Signals

Throughout the different phases of commissural axon guidance, two alternatively spliced variants of the *Robo3* transcript, *Robo3.1* and *Robo3.2*, are expressed (Chen et al., 2008). Before axons cross through the spinal cord midline, only Robo3.1 protein is expressed and no Robo3.2 protein is detected despite the abundance of *Robo3.2* mRNA at this stage (Chen et al., 2008). However, after the axons cross the floor plate, Robo3.2 protein is detected, and seen exclusively in the postcrossing segment of these axons (Figure 1A, right panel).

A major difference between these two isoforms is that *Robo3.2* is a predicted NMD target. The *Robo3.2* isoform differs from *Robo3.1* by the presence of a retained intron. The *Robo3* gene contains 27 introns, which are all spliced out in *Robo3.1*. However, in *Robo3.2*, intron 26 is retained, resulting in the appearance of a new intron-derived stop codon (Figure 1A). An exon junction complex, which derives from the splicing of intron 27, is downstream of the new stop codon in *Robo3.2*, which makes this isoform an NMD target. We therefore wondered if NMD contributes to the precise spatiotemporal regulation of Robo3.2 expression during axon guidance.

Since NMD targets transcripts when they are initially translated, we first wanted to establish how Robo3.2 protein expression is induced. We considered two models: the expression of Robo3.2 could be temporally programmed to coincide with the time when axons cross the midline (~E11), or the expression of Robo3.2 could be induced when the axons encounter the floor plate. To address this, we used spinal cord “half open book” explant cultures. Half open book explants were dissected from mouse embryos at embryonic day (E) 10.5, a time point before commissural axons have reached the floor plate.

We first sought to confirm that the half open book culture recapitulates axonal expression patterns that are floor plate-dependent. Half open book explants were prepared in a way that each lateral half was harvested either with or without the floor plate (referred as +FP or −FP throughout the text, Figure 1B). Previous studies have utilized this system to examine floor plate-dependent changes in axonal behavior (Zou et al., 2000). As expected, axons from −FP explants expressed TAG-1, a marker for precrossing axons (Figure S1A). These axons did not express postcrossing marker L1 (Figure S1A). However, axons from +FP explants no longer expressed TAG-1, but instead exhibited L1 staining (Figure S1A). These data indicate that the half open book culture recapitulates the expression patterns that are regulated by the floor plate in vivo.

We next examined whether the floor plate induces Robo3.2 expression. Robo3.2 levels were measured in half open book axons at DIV2 using a Robo3.2-specific antibody (Chen et al., 2008). Robo3.2 staining was undetectable in −FP cultures, while Robo3.2 was readily detected in axons of +FP cultures (Figure 1C). In contrast to Robo3.2, Robo3.1 was detected in axons of −FP explants, while Robo3.1 was not detectable in +FP cultures (Figures 1C and 1D). Thus, these data indicate that the expression of Robo3.2 is induced by the floor plate.

We next asked if the floor plate is sufficient to induce Robo3.2 protein in commissural axons. To test this, we prepared conditioned media from isolated floor plate tissue (Nawabi et al., 2010) (Figure 1E). Application of floor plate-conditioned media (FCM) to −FP explants resulted in pronounced Robo3.2 protein in axons, while control media did not induce Robo3.2 expression (Figure 1F). Robo3.2 induction was most prominent at the most

distal parts of the axons, suggesting that the regulatory pathways controlling Robo3.2 expression may be enriched in distal axons (Figure 1G-H).

Intriguingly, Robo3.2 protein was also induced in commissural cell bodies by FCM (Figure S1B). In vivo, Robo3.2 expression is only seen in the postcrossing segment of commissural axons. The limited expression of Robo3.2 in vivo supports the idea that the floor plate mediates local induction of Robo3.2 since only the axons are exposed to floor plate in vivo. Taken together, these data show that the floor plate is necessary as well as sufficient for Robo3.2 induction in commissural neurons.

Robo3.2 mRNA Is Translationally Repressed Prior to Midline Crossing

We next asked if the undetectable levels of Robo3.2 protein in precrossing axons is due to degradation of *Robo3.2* mRNA by NMD. NMD targets are typically subjected to mRNA degradation. However, the *Robo3.2* transcript appears to be relatively abundant in commissural cells (Chen et al., 2008) (Figure S2A), which suggests that it escapes NMD in the cell body. Nevertheless, we asked if NMD contributes to the stability of *Robo3.2* transcripts in precrossing neurons. A widely used approach to determine if a transcript is subjected to NMD is to determine if it accumulates after treatment of cells with cycloheximide, a protein synthesis inhibitor (Carter et al., 1995). This accumulation occurs because NMD-dependent RNA degradation requires protein translation (Ishigaki et al., 2001). We applied cycloheximide for 4 hr to −FP explants and measured *Robo3.2* levels in these explants by qRT-PCR. *Arc*, an established NMD target (Giorgi et al., 2007), was increased by 2.5-fold following cycloheximide treatment (Figure 2A). In contrast, *Robo3.2* levels were unaffected by this treatment (Figure 2A). Similarly, *Robo3.1*, which is not a predicted NMD target, was unaffected by cycloheximide treatment. These findings indicate that suppression of Robo3.2 protein levels is not due to NMD at this developmental stage.

We next asked why *Robo3.2* is not subjected to NMD. Because NMD is dependent on translation, *Robo3.2* might escape NMD if it is not translated in precrossing neurons. To test this possibility, we isolated polysome-bound and polysome-free mRNAs by 10-50% sucrose gradient fractionation. FMRP, a marker of actively translating ribosomes, was selectively detected in the polysome fractions by western blotting (Figure 2B). Similarly, *Robo3.1* transcripts were detected in the polysome fractions by RT-PCR (Figure 2B). However, *Robo3.2* transcripts were only detected in the lighter fractions, which contain non-translating mRNAs (Figure 2B). These data demonstrate that *Robo3.2* is translationally silenced in precrossing neurons.

As a further control, we asked if Robo3.2 protein is subjected to proteasomal degradation in precrossing neurons. To test this, we treated −FP explants with the proteasome inhibitor MG-132. Treatment with proteasome inhibitors failed to increase Robo3.2 levels in -FP explants (Figure S2B). These data further indicate that the absence of Robo3.2 protein at this stage reflects translational suppression rather than a posttranslational mechanism.

Robo3.2 mRNA Is Transported into Precrossing and Postcrossing Axons

Since NMD occurs after a transcript is translated, we sought to determine how *Robo3.2* translation is initiated. Because Robo3.2 expression is spatially restricted to postcrossing axons, and FCM results in highly selective expression of Robo3.2 in distal axons, we considered the possibility that *Robo3.2* is locally translated (Figure 1F). We therefore first examined if *Robo3.2* mRNA is localized to axons. Riboprobes directed against *Robo3.2* exhibited punctate localization along the axons, with enrichment towards the distal axons (Figures 3A-D). This localization was seen in both pre- and postcrossing axons. Sense

riboprobes and *Robo3.1*-specific riboprobes did not show signals in axons of either −FP or +FP explants (Figures S3A and S3B).

To further confirm that *Robo3.2* transcripts are localized to axons, we performed RT-PCR in isolated commissural axons (Figures 3E and 3F). To purify axons, we cultured explants in microfluidic chambers (Taylor et al., 2005). In these devices, explants are cultured in the cell body compartment, and axons grow through a 450 μm microgroove barrier and appear in the axonal compartment by DIV4. Consistent with the FISH data, *Robo3.2* mRNA was detected both in axons and cell bodies by RT-PCR, while *Robo3.1* transcripts were only detected in cell bodies (Figure 3F). Quantitative RT-PCR data from isolated axonal samples further confirmed that *Robo3.2* mRNA is present in −FP and +FP axons (Figure 3G). These data demonstrate that *Robo3.2* mRNA is trafficked to axons before and after crossing the midline.

Similar to cell bodies, the undetectable levels of Robo3.2 protein in precrossing axons was not due to NMD as selective treatment of axons with cycloheximide in microfluidic chambers did not result in an increase in *Robo3.2* mRNA levels in these axons (Figure S3C).

Robo 3.2 is Locally Translated in Postcrossing Axons

We next asked if *Robo3.2* is translated in axons. To address this, we monitored Robo3.2 levels after selectively inhibiting protein translation in axons. We cultured +FP explants in microfludic chambers to fluidically isolate axons from cell bodies. This approach allows chemical treatments to only affect axons without affecting cell bodies (Cohen et al., 2011; Taylor et al., 2005). Selective application of cycloheximide to axons for 12 hr resulted in a nearly complete absence of Robo3.2 expression (Figures 4A and 4B). These data support the idea that Robo3.2 levels are regulated by local translation.

We next asked if FCM induces the intra-axonal synthesis of *Robo3.2*. To test this, axons in −FP explant cultures were transected to prevent the possibility of transport of Robo3.2 protein from the cell body and were treated with FCM (Figure 4C). Treatment of severed axons with FCM resulted in the appearance of Robo3.2, with particular enrichment in the distal parts of the axons (Figure 4D). This effect was blocked by co-application of cycloheximide indicating that the induction of Robo3.2 does not require the cell body and therefore is due to intra-axonal translation.

To further establish if FCM induces translation of *Robo3.2* mRNA, we examined if this treatment causes *Robo3.2* transcripts to shift to polysomes. Treatment of −FP explants with FCM resulted in the appearance of *Robo3.2* mRNA in polysomes (Figure S4A), indicating that *Robo3.2* is translationally derepressed upon exposure to floor plate signals.

To determine if contact to the floor plate itself induces Robo3.2 synthesis in axons, we used half open book explants prepared from Wallerian degeneration slow (Wld^S) mice. The Wld^S mutant mouse contains a triplicate repeat of the *NMNAT-1* gene fused to the N-terminal domain of the ubiquitin ligase *UBE4* gene (Perry et al., 1991). Overexpression of Wld^S markedly delays axonal degeneration after axotomy (Feng et al., 2010). Because axons from Wld^S animals are viable following transection without exhibiting morphological signs of degeneration, they can be used to examine the role of local translation in isolated axons over prolonged periods. We cultured +FP explants from E10.5 Wld^S embryos, and then cut the explants at DIV0.5 so that the cell bodies were severed from the axons (Figure 4E). Transected axons were capable of growing through the floor plate and inducing Robo3.2 after crossing the midline in the absence of cell bodies (Figure 4F). As a control, we confirmed that the severing procedure removed the cell bodies from these explants (Figures S4B and S4C).

Taken together, these data indicate that *Robo3.2* translation occurs in axons in response to floor plate signals. Because NMD-mediated degradation is translation dependent, this finding suggests that NMD-dependent regulation of *Robo3.2* mRNA would only occur in the postcrossing segment of commissural axons.

Robo3.2 is Targeted for NMD upon Translational Derepression

In order to determine if *Robo3.2* is potentially regulated by NMD, we next asked if NMD machinery proteins are bound to *Robo3.2* transcripts. We used RNA immunoprecipitation (RIP) to examine the physical interaction of Upf1 and Upf2 with *Robo3.2 mRNA* in +FP explants. mRNAs that are targeted by NMD have Upf2 bound to exon junction complexes. Upf2-bound mRNAs trigger NMD by recruiting Upf1. Both Upf2 and Upf1 proteins interact with *Robo3.2* transcripts (Figure S5A) suggesting that *Robo3.2* mRNA is a potential NMD target in commissural neurons.

We next asked if *Robo3.2* mRNA is subjected to NMD when commissural neurons begin to translate *Robo3.2* upon exposure to floor plate signals. To address this, we measured *Robo3.2* levels by qRT-PCR after treatment with FCM. Following treatment with FCM, *Robo3.2* transcript levels were reduced by 70% in commissural cell bodies compared to treatment with control media (Figure 5A). This effect was blocked by cycloheximide, suggesting that *Robo3.2* mRNA gets degraded following its translation induced by floor plate signals (Figure 5A). Interestingly, *Robo3.1* levels drop upon FCM treatment. This is expected because *Robo3.1* mRNA is downregulated when axons cross the midline (Chen et al., 2008), presumably via a transcriptional mechanism. FCM-mediated drop in *Robo3.1* levels was not affected by cycloheximide, since this is not mediated by NMD (Figure 5A). These data suggest that *Robo3.2* mRNA becomes a substrate for NMD when its translation is induced.

To ensure that translation-dependent degradation of *Robo3.2* mRNA involves NMD, we repeated this experiment in NMD-deficient commissural neurons. We used *Upf2* conditional knockout mouse (Weischenfeldt et al., 2008) expressing *Wnt1-Cre* to ablate *Upf2* expression selectively in dorsal commissural neurons (*Wnt1-Cre*; $Upf2^{fl/fl}$).We prepared −FP explants from *Wnt1-Cre*; $Upf2^{fl/fl}$ (*Upf2* cKO) embryos and treated these explants with FCM (Figure S5B). Unlike in control explants (Figure 5A), FCM did not result in decreased *Robo3.2* transcript levels in NMD-deficient neurons. This confirms that *Robo3.2* degradation occurs in an NMD-dependent manner. Taken together, these experiments indicate that *Robo3.2* mRNA becomes a substrate for NMD when its translation is induced in axons.

NMD Components Are Enriched in Axonal Growth Cones

We next examined whether axons have the capacity to utilize NMD. NMD components have not been previously described in axons. Staining of distal commissural axons with antibodies specific for Upf2 and Upf1 revealed selective labeling of distal axons (Figures 5B and 5C). As with Upf1 and Upf2, staining with an antibody specific for Smg1, a kinase required for NMD, revealed selective enrichment in the distal-most portion of these axons (Figure 5D). Western blot of these proteins in isolated axons further confirmed that commissural axons contain components of NMD machinery (Figure S5F). Taken together, these findings suggest that NMD might have functional roles in commissural axons.

NMD Regulates Robo3.2 Protein Levels in Postcrossing Axons

We first examined whether NMD is required for the floor plate-dependent induction of Robo3.2. As with control explants, −FP explants exhibited minimal, and +FP explants exhibited readily detectable Robo3.2 expression in *Upf2* cKO embryos (Figures S5G and

S5H), indicating that NMD is not involved in either repression or induction of Robo3.2 during midline crossing.

We next examined if NMD affects the levels of Robo3.2 expression in commissural axons. We examined the effect of *Upf2* cKO on the levels of Robo3.2 protein induction following treatment with FCM. −FP explants from both control and *Upf2* cKO embryos were treated with FCM and Robo3.2 levels were measured by immunofluorescence (Figures 5E and 5F). Following treatment with FCM Robo3.2 was induced in axons from both control and *Upf2* cKO explants (Figure 5E). However, Robo3.2 staining was nearly 2-fold increased in axons from *Upf2* cKO explants (Figure 5F). This effect was also observed in transected axons that received FCM, confirming that the increase in Robo3.2 derives from local translation (Figures 5G and S6A-B').

We next monitored Robo3.2 expression in axons that contact the floor plate in *Upf2* cKO explants. Contact with the floor plate provides a more physiologically relevant stimulus than FCM. Staining of axons from +FP explants indicated that Robo3.2 levels were 3.5-fold higher in *Upf2* cKO explants compared to controls (Figures 5H and 5I). Taken together, these data indicate that NMD limits the amount of Robo3.2 protein in axons exposed to floor plate signals.

We next asked if the higher Robo3.2 levels in axons are due to increased stability of *Robo3.2* mRNAs in axons. We measured *Robo3.2* mRNA levels in axons from control and *Upf2* cKO explants. We treated −FP axons of control and *Upf2 cKO* explants in microfluidic chambers with FCM (Figure 5J). We also used NMD-deficient axons by testing isolated +FP axons from *Upf2* cKO explants (Figure 5J). In both cases, *Robo3.2* mRNA levels were found to be higher in *Upf2* cKO axons compared to control axons. Taken together, these data indicate that axonal *Robo3.2* transcripts are degraded by NMD, which limits Robo3.2 protein levels in postcrossing axons.

As a control, we examined if the increased levels of Robo3.2 protein in *Upf2* cKO commissural axons could be due to an overall increase in the level of *Robo3.2* mRNA in cell bodies. We measured *Robo3.2* mRNA levels in control and *Upf2* cKO commissural cell bodies at E13.5. *Robo3.2* mRNA levels were not significantly affected in the commissural cell bodies of *Upf2* cKO compared to controls (Figure S6C). These data are consistent with the idea that the upregulation of Robo3.2 protein in Upf2-deficient axons is not due to an overall increase in *Robo3.2* mRNA levels in cell bodies (Figure S6C).

NMD Regulates Postcrossing Axon Behavior

We next sought to investigate if NMD influences commissural axon guidance during development. Dorsal commissural axons are initially attracted to the midline. After crossing the midline, they exert a more complicated trajectory with respect to the distance from the midline (Kadison and Kaprielian, 2004). While only a small portion of the postcrossing axons (medial longitudinal commissural, MLC) remain adjacent to the midline, the majority (intermediate longitudinal commissural, ILC) travel away from the midline, and project diagonally before ascending in the spinal cord (Jaworski et al., 2010; Kadison and Kaprielian, 2004) (Figure 6A).

To address the potential function of NMD in commissural axon guidance, we analyzed commissural axon trajectories in *Upf2* cKO embryos. To assess axon trajectories, the lipophilic tracer DiI was injected into E13.5 spinal cords, and axons were analyzed after the entire axon was uniformly labeled with DiI. *Upf2* cKO axons exhibited normal precrossing behavior but displayed more lateral trajectories on the contralateral side compared to control axons (Figure 6B). To measure the lateral distribution, the ascending axons were binned into

three categories based on their distance from the midline: 0-75 μm, 75-275 μm, and >275 μm (Figures 6A and 6B). In *Upf2* cKO embryos, the proportions of postcrossing axons in the 0-75 μm and 75-275 μm categories were significantly reduced, while the proportion in the >275 μm category was significantly increased (Figure 6C). Additionally, *Upf2* cKO axons exhibited disorganized trajectories with several sudden turns and path changes (Figure 6D).

To further confirm the phenotype of NMD-deficient neurons, we electroporated a dominant-negative Upf1 construct (hUpf1K498A) in E10.5 open book explants (Figure 6E). As with the *Upf2* cKO neurons, expression of dominant-negative Upf1 resulted in lateral positioning of the axonal trajectories (Figures 6F and 6G). The increased lateral distribution of postcrossing axons is consistent with over-repulsion from the midline due to excessive levels of Robo3.2. Taken together, these data indicate that NMD is required for the proper guidance of postcrossing axons.

Since Robo1 and Robo2 influence postcrossing trajectories, we asked if their expression was altered in *Upf2* cKO axons. qRT-PCR showed that *Robo1* and *Robo2* transcripts are not affected in *Upf2* cKO neurons compared to control neurons (Figure S6D) suggesting that misregulation of Robo1 and Robo2 are unlikely to contribute to the guidance defects in NMD-deficient neurons.

Localization of NMD Machinery in Growth Cones Is a Feature of Various Types of Neurons

We next asked if local regulation of mRNA stability by NMD could occur in axons of other neuronal types. We performed immunostainings for Upf2, Upf1 and Smg1on P1 DIV7 rat hippocampal and E14 rat dorsal root ganglia (DRG) neurons (Figure 7). Similar to commissural neurons, all of these proteins were highly enriched in growth cones of both neuronal types (Figure 7C).

Although Robo3 has major roles in the guidance of commissural axons, Robo3 is not expressed in many neurons and has no described functions in hippocampal and sensory neurons (Sabatier et al., 2004). However, other NMD targets are likely to exist in neurons. For example, at least 152 predicted NMD targets were predicted based on the presence of spliced introns in the 3′ UTR (Giorgi et al., 2007). These data suggest that the local utilization of NMD to regulate mRNA stability and protein levels in growth cones may be a common feature of diverse neuronal types.

DISCUSSION

Our study identifies intra-axonal NMD as a mechanism that regulates axon guidance. We find that proteins that are involved in NMD display substantial enrichment in growth cones in various diverse types of neurons. This localization suggests that NMD may function locally within growth cones to regulate local protein expression. Our data indicate that NMD regulates the levels of Robo3.2 in growth cones, and thereby influences the chemotropic properties of growth cones and their axonal trajectories after midline crossing.

Role of NMD in Regulating Robo3.2 and Postcrossing Axon Trajectories

Our data demonstrate that transcripts can evade NMD by translational repression. Our polysome profiling experiments suggest that *Robo3.2* transcripts are translationally repressed in cell bodies and precrossing axons. When the axon encounters the floor plate, *Robo3.2* is derepressed resulting in local synthesis and enabling surveillance by the NMD machinery within the distal axon. Thus the initial round of translation, which typically occurs on nascent mRNA, occurs locally within axons after *Robo3.2* is translationally

derepressed by the floor plate (Figure S7C). NMD-dependent degradation of *Robo3.2* transcripts limits Robo3.2 levels, potentially to a single Robo3.2 per targeted mRNA.

Our data indicate that the proper guidance of postcrossing commissural axons requires NMD. NMD-deficient postcrossing axons exhibit elevated Robo3.2 levels and over-repulsion from the midline in vivo. This is consistent with previous studies showing that overexpression of Robo3.2 in precrossing neurons leads to repulsion of axons from the midline (Chen et al., 2008). NMD-dependent control of Robo3.2 levels is likely to contribute to the overall level of axonal repulsion from the midline, ensuring proper lateral positioning of the axons during ascension in the spinal cord. However, NMD is likely to have additional targets in axons. Cell adhesion molecules and cytoskeletal molecules are known to regulate axon guidance (Vitriol and Zheng, 2012). Conceivably, physiological regulation of transcripts encoding these or other proteins by axonal NMD may influence axonal trajectories.

Potential Role of Robo3.2 in Postcrossing Axons of Dorsal Commissural Neurons

Axons of dorsal commissural neurons sort into specific mediolateral positions in the contralateral side after crossing the midline (Imondi and Kaprielian, 2001; Jaworski et al., 2010; Kadison and Kaprielian, 2004). While the minority of the postcrossing axons remains in the longitudinal track adjacent to the midline (MLC), the majority project diagonally away from the midline to varying lateral positions (ILC). We find that the absence of NMD results in a reduction in MLC trajectories, consistent with them adopting a more diagonal trajectory, as well as a lateral shift in the ILC trajectories. These trajectory shifts are consistent with over-repulsion from the midline.

During midline crossing, Robo proteins contribute to distinct guidance decisions (Evans and Bashaw, 2010; Jaworski et al., 2010; Spitzweck et al., 2010). Robo1 ensures that all commissural axons leave the midline, while Robo2 is required for the initiation of the diagonal trajectories in mouse spinal cord (Jaworski et al., 2010; Reeber et al., 2008). The role of Robo2 in diagonal trajectories is supported by the finding that postcrossing axons remain adjacent to the midline in *Robo2*−/−spinal cord. Robo3.2 appears to enhance the activity of Robo2 since knockdown of Robo3.2 reduces Robo1/2-mediated repulsion from the midline (Chen et al., 2008). However, it is not clear what determines the degree of the repulsion from the midline during diagonal trajectories. Our findings suggest the possibility that the level of Robo3.2 in postcrossing axons may determine the degree of repulsion from the midline. While the MLC axons and ILC axons in close proximity to the midline might have moderate levels of Robo3.2, the more lateral ILC axons may have higher Robo3.2 ensuring proper lateral positioning. An intriguing possibility is that the level of NMD activity may vary in different axons, resulting in different levels of axonal Robo3.2 and lateral positioning.

Local NMD as a Regulator of Local Translation

We also find that the growth cone is a site for local NMD in neurons. NMD has previously been shown to regulate the expression *Arc* transcripts in hippocampal neurons in response to synaptic stimulation (Giorgi et al., 2007). However, the possibility of local regulation of *Arc* transcripts by NMD within dendrites or spines was not examined. Our data suggest that NMD can function locally to regulate the translation of local mRNA pools. Conceivably, NMD may have important roles in the regulation of local translation pathways in dendritic spines, which are regions that are also characterized by high levels of local translation (Bramham and Wells, 2007; Sutton and Schuman, 2006). The high degree of enrichment of NMD proteins in growth cones suggests that NMD may influence axonal mRNAs that affect various growth cone functions. Apart from NMD, Upf1 is also involved in Staufen-mediated

mRNA decay (SMD) (Kim et al., 2005). Thus, axonally localized Upf1 may also influence the translation of SMD targets.

Our data demonstrate that local translation is regulated by mechanisms that control mRNA stability in axons. Pathways that induce mRNA degradation can limit the total amount of protein that can be translated. The expression of NMD proteins in growth cones of diverse neuronal types suggests that this may be a recurrent mechanism used to influence local translation pathways.

Local Translation Regulates the Pathfinding Behavior of Growth Cones at the Floor Plate

Our data also provide insight into the mechanism by which the floor plate alters chemotropic responses of axons. A previous study by Flanagan and colleagues (Brittis et al., 2002), initially raised the possibility that local translation could affect the chemotropic properties of growth cones by showing that the midline could induce the translation of a reporter construct containing the 3′UTR of *EphA2*. However, the endogenous *EphA2* transcript was not detected in commissural axons, and no endogenous transcripts that are translated in response to exposure to the floor plate were identified. Our data demonstrate the first endogenous transcript that is locally translated in response to the floor plate.

It remains unclear which floor plate-derived factor triggers axonal translation of *Robo3.2*. Well-known floor plate cues, netrin-1, sonic hedgehog and NrCAM, do not induce Robo3.2 protein in commissural axons (D.C and S.R.J., unpublished data). Because floor plate-conditioned media is capable of inducing Robo3.2 synthesis, the responsible factor may be a secreted molecule. However, floor plate-conditioned media may contain ectodomains of surface or transmembrane proteins shed following cleavage by membrane-associated proteases. Indeed, a recent study found that the transmembrane protein NrCAM accumulates in floor plate-conditioned media (Nawabi et al., 2010). Therefore, physiologic induction of Robo3.2 synthesis may be mediated by contact of axons with membrane-bound proteins in floor plate cells.

EXPERIMENTAL PROCEDURES

Mice and Constructs

Explant cultures were prepared from CD1 mouse embryos (Charles River Laboratories), *Upf2* cKO mice (Weischenfeldt et al., 2008), or C57BL/6OlaHsd-Wld^{s} mice (Harlan). In experiments using *Upf2* deletion in commissural neurons *Upf2* conditional knockout mice were crossed with *Wnt1-Cre* mice (Matsumoto et al., 2007), and *Wnt1-Cre*; *Upf2*$^{fl/fl}$ or *Wnt1-Cre*; *Upf2*$^{wt/wt}$ embryos were used. The hUpf1 K498A dominant negative expression vector was a gift from Jens Lykke-Andersen (University of California, San Diego) and was co-electroporated with an EGFP-expressing plasmid in order to identify the transfected neurons.

Explant Cultures and Reagents

Open book explant cultures were prepared from E10.5 thoracic spinal cords as previously described (Moore and Kennedy, 2008). Floor plate-conditioned media was prepared by culturing thoracic spinal cord floor plate from 20 E10.5 embryos (200 explants) in 300 μl Neurobasal media. The conditioned media was collected after 36 hr, and the entire 300 μl was applied to axons. Microfluidic chambers were prepared as described previously (Cohen et al., 2011; Hengst et al., 2009; Taylor et al., 2005). For additional details, see the Extended Experimental Procedures.

Immunofluorescence, RNA Preparation and Expression Analysis

Half open book explants were fixed in 4% paraformaldehyde prior to immunostaining with antibodies specific to Robo3.1 and Robo3.2 (Genentech). Immunofluorescence was acquired on a Zeiss LSM 510 confocal microscopy and processed with LSM 5 image examiner. RNA was prepared using TRIzol (Invitrogen). RT-PCR was performed using SuperScript III (Invitrogen). For additional details, see the Extended Experimental Procedures.

Data Analysis

Statistical analysis was performed using Student's t-test and is reported as mean ± SEM. When comparing different treatments on wild type explants, we considered the samples as two samples with equal variance. When comparing mutant tissue with control littermates, we considered the samples as two samples with unequal variance. In all cases, 2-tailed distribution parameter was applied.

Supplementary Material

Refer to Web version on PubMed Central for supplementary material.

Acknowledgments

We thank Dr. Jens Lykke-Andersen for generously providing the hUpf1K498A construct, anti-Upf1 and anti-Upf2 antibodies, Dr. S. Blanchard and L. Wang for equipments and helpful suggestions regarding the polysome experiments, S. Kadison for advice on DiI labeling, and M. Tessier-Lavigne and Genentech for sharing Robo3.1- and Robo3.2-specific antibodies. We also thank members of the Jaffrey lab for helpful comments and suggestions. This work was supported by NIH grant NS56306 to S.R.J and a European Molecular Biology Organization (EMBO) postdoctoral fellowship to D.C.

REFERENCES

Black DL, Zipursky SL. To cross or not to cross: alternatively spliced forms of the Robo3 receptor regulate discrete steps in axonal midline crossing. Neuron. 2008; 58:297–298. [PubMed: 18466738]

Bramham CR, Wells DG. Dendritic mRNA: transport, translation and function. Nat Rev Neurosci. 2007; 8:776–789. [PubMed: 17848965]

Brittis PA, Lu Q, Flanagan JG. Axonal protein synthesis provides a mechanism for localized regulation at an intermediate target. Cell. 2002; 110:223–235. [PubMed: 12150930]

Campbell DS, Holt CE. Chemotropic responses of retinal growth cones mediated by rapid local protein synthesis and degradation. Neuron. 2001; 32:1013–1026. [PubMed: 11754834]

Carter MS, Doskow J, Morris P, Li S, Nhim RP, Sandstedt S, Wilkinson MF. A regulatory mechanism that detects premature nonsense codons in T-cell receptor transcripts in vivo is reversed by protein synthesis inhibitors in vitro. J Biol Chem. 1995; 270:28995–29003. [PubMed: 7499432]

Chang YF, Imam JS, Wilkinson MF. The nonsense-mediated decay RNA surveillance pathway. Annu Rev Biochem. 2007; 76:51–74. [PubMed: 17352659]

Chen Z, Gore BB, Long H, Ma L, Tessier-Lavigne M. Alternative splicing of the Robo3 axon guidance receptor governs the midline switch from attraction to repulsion. Neuron. 2008; 58:325–332. [PubMed: 18466743]

Cohen MS, Bas Orth C, Kim HJ, Jeon NL, Jaffrey SR. Neurotrophin-mediated dendrite-to-nucleus signaling revealed by microfluidic compartmentalization of dendrites. Proc Natl Acad Sci U S A. 2011; 108:11246–11251. [PubMed: 21690335]

Doma MK, Parker R. RNA quality control in eukaryotes. Cell. 2007; 131:660–668. [PubMed: 18022361]

Dostie J, Dreyfuss G. Translation is required to remove Y14 from mRNAs in the cytoplasm. Curr Biol. 2002; 12:1060–1067. [PubMed: 12121612]

Evans TA, Bashaw GJ. Functional diversity of Robo receptor immunoglobulin domains promotes distinct axon guidance decisions. Curr Biol. 2010; 20:567–572. [PubMed: 20206526]

Feng Y, Yan T, He Z, Zhai Q. Wld(S), Nmnats and axon degeneration--progress in the past two decades. Protein Cell. 2010; 1:237–245. [PubMed: 21203970]

Giorgi C, Yeo GW, Stone ME, Katz DB, Burge C, Turrigiano G, Moore MJ. The EJC factor eIF4AIII modulates synaptic strength and neuronal protein expression. Cell. 2007; 130:179–191. [PubMed: 17632064]

Hengst U, Deglincerti A, Kim HJ, Jeon NL, Jaffrey SR. Axonal elongation triggered by stimulus-induced local translation of a polarity complex protein. Nat Cell Biol. 2009; 11:1024–1030. [PubMed: 19620967]

Hodgkin J, Papp A, Pulak R, Ambros V, Anderson P. A new kind of informational suppression in the nematode Caenorhabditis elegans. Genetics. 1989; 123:301–313. [PubMed: 2583479]

Imondi R, Kaprielian Z. Commissural axon pathfinding on the contralateral side of the floor plate: a role for B-class ephrins in specifying the dorsoventral position of longitudinally projecting commissural axons. Development. 2001; 128:4859–4871. [PubMed: 11731465]

Ishigaki Y, Li X, Serin G, Maquat LE. Evidence for a pioneer round of mRNA translation: mRNAs subject to nonsense-mediated decay in mammalian cells are bound by CBP80 and CBP20. Cell. 2001; 106:607–617. [PubMed: 11551508]

Jaworski A, Long H, Tessier-Lavigne M. Collaborative and specialized functions of Robo1 and Robo2 in spinal commissural axon guidance. J Neurosci. 2010; 30:9445–9453. [PubMed: 20631173]

Jung H, Yoon BC, Holt CE. Axonal mRNA localization and local protein synthesis in nervous system assembly, maintenance and repair. Nat Rev Neurosci. 2012; 13:308–324. [PubMed: 22498899]

Kadison SR, Kaprielian Z. Diversity of contralateral commissural projections in the embryonic rodent spinal cord. J Comp Neurol. 2004; 472:411–422. [PubMed: 15065116]

Kim YK, Furic L, Desgroseillers L, Maquat LE. Mammalian Staufen1 recruits Upf1 to specific mRNA 3′UTRs so as to elicit mRNA decay. Cell. 2005; 120:195–208. [PubMed: 15680326]

Leeds P, Wood JM, Lee BS, Culbertson MR. Gene products that promote mRNA turnover in Saccharomyces cerevisiae. Mol Cell Biol. 1992; 12:2165–2177. [PubMed: 1569946]

Lejeune F, Maquat LE. Mechanistic links between nonsense-mediated mRNA decay and pre-mRNA splicing in mammalian cells. Curr Opin Cell Biol. 2005; 17:309–315. [PubMed: 15901502]

Leung KM, van Horck FP, Lin AC, Allison R, Standart N, Holt CE. Asymmetrical beta-actin mRNA translation in growth cones mediates attractive turning to netrin-1. Nat Neurosci. 2006; 9:1247–1256. [PubMed: 16980963]

Li S, Wilkinson MF. Nonsense surveillance in lymphocytes? Immunity. 1998; 8:135–141. [PubMed: 9491995]

Long H, Sabatier C, Ma L, Plump A, Yuan W, Ornitz DM, Tamada A, Murakami F, Goodman CS, Tessier-Lavigne M. Conserved roles for Slit and Robo proteins in midline commissural axon guidance. Neuron. 2004; 42:213–223. [PubMed: 15091338]

Maquat LE, Kinniburgh AJ, Rachmilewitz EA, Ross J. Unstable beta-globin mRNA in mRNA-deficient beta o thalassemia. Cell. 1981; 27:543–553. [PubMed: 6101206]

Matsumoto Y, Irie F, Inatani M, Tessier-Lavigne M, Yamaguchi Y. Netrin-1/DCC signaling in commissural axon guidance requires cell-autonomous expression of heparan sulfate. J Neurosci. 2007; 27:4342–4350. [PubMed: 17442818]

McGlincy NJ, Smith CW. Alternative splicing resulting in nonsense-mediated mRNA decay: what is the meaning of nonsense? Trends Biochem Sci. 2008; 33:385–393. [PubMed: 18621535]

Moore SW, Kennedy TE. Dissection and culture of embryonic spinal commissural neurons. Curr Protoc Neurosci. 2008 Chapter 3, Unit 3 20.

Nawabi H, Briancon-Marjollet A, Clark C, Sanyas I, Takamatsu H, Okuno T, Kumanogoh A, Bozon M, Takeshima K, Yoshida Y, et al. A midline switch of receptor processing regulates commissural axon guidance in vertebrates. Genes Dev. 2010; 24:396–410. [PubMed: 20159958]

O'Donnell M, Chance RK, Bashaw GJ. Axon growth and guidance: receptor regulation and signal transduction. Annu Rev Neurosci. 2009; 32:383–412. [PubMed: 19400716]

Perry VH, Brown MC, Lunn ER. Very Slow Retrograde and Wallerian Degeneration in the CNS of C57BL/Ola Mice. Eur J Neurosci. 1991; 3:102–105. [PubMed: 12106273]

Reeber SL, Sakai N, Nakada Y, Dumas J, Dobrenis K, Johnson JE, Kaprielian Z. Manipulating Robo expression in vivo perturbs commissural axon pathfinding in the chick spinal cord. J Neurosci. 2008; 28:8698–8708. [PubMed: 18753371]

Serafini T, Kennedy TE, Galko MJ, Mirzayan C, Jessell TM, Tessier-Lavigne M. The netrins define a family of axon outgrowth-promoting proteins homologous to C. elegans UNC-6. Cell. 1994; 78:409–424. [PubMed: 8062384]

Spitzweck B, Brankatschk M, Dickson BJ. Distinct protein domains and expression patterns confer divergent axon guidance functions for Drosophila Robo receptors. Cell. 2010; 140:409–420. [PubMed: 20144763]

Sutton MA, Schuman EM. Dendritic protein synthesis, synaptic plasticity, and memory. Cell. 2006; 127:49–58. [PubMed: 17018276]

Taylor AM, Blurton-Jones M, Rhee SW, Cribbs DH, Cotman CW, Jeon NL. A microfluidic culture platform for CNS axonal injury, regeneration and transport. Nat Methods. 2005; 2:599–605. [PubMed: 16094385]

Tennyson VM. The fine structure of the axon and growth cone of the dorsal root neuroblast of the rabbit embryo. J Cell Biol. 1970; 44:62–79. [PubMed: 5409464]

Vitriol EA, Zheng JQ. Growth cone travel in space and time: the cellular ensemble of cytoskeleton, adhesion, and membrane. Neuron. 2012; 73:1068–1081. [PubMed: 22445336]

Weischenfeldt J, Damgaard I, Bryder D, Theilgaard-Monch K, Thoren LA, Nielsen FC, Jacobsen SE, Nerlov C, Porse BT. NMD is essential for hematopoietic stem and progenitor cells and for eliminating by-products of programmed DNA rearrangements. Genes Dev. 2008; 22:1381–1396. [PubMed: 18483223]

Weischenfeldt J, Waage J, Tian G, Zhao J, Damgaard I, Jakobsen JS, Kristiansen K, Krogh A, Wang J, Porse BT. Mammalian tissues defective in nonsense-mediated mRNA decay display highly aberrant splicing patterns. Genome Biol. 2012; 13:R35. [PubMed: 22624609]

Zhang J, Sun X, Qian Y, LaDuca JP, Maquat LE. At least one intron is required for the nonsense-mediated decay of triosephosphate isomerase mRNA: a possible link between nuclear splicing and cytoplasmic translation. Mol Cell Biol. 1998; 18:5272–5283. [PubMed: 9710612]

Zheng S, Gray EE, Chawla G, Porse BT, O'Dell TJ, Black DL. PSD-95 is post-transcriptionally repressed during early neural development by PTBP1 and PTBP2. Nat Neurosci. 2012; 15:381–388. S381. [PubMed: 22246437]

Zou Y, Stoeckli E, Chen H, Tessier-Lavigne M. Squeezing axons out of the gray matter: a role for slit and semaphorin proteins from midline and ventral spinal cord. Cell. 2000; 102:363–375. [PubMed: 10975526]

HIGHLIGHTS

- Robo3.2 is locally synthesized in growth cones of commissural axons
- NMD proteins are enriched in growth cones of diverse types of neurons
- NMD regulates the amount of Robo3.2 synthesized in growth cones
- Defects in NMD lead to abnormal axonal trajectories in spinal cord

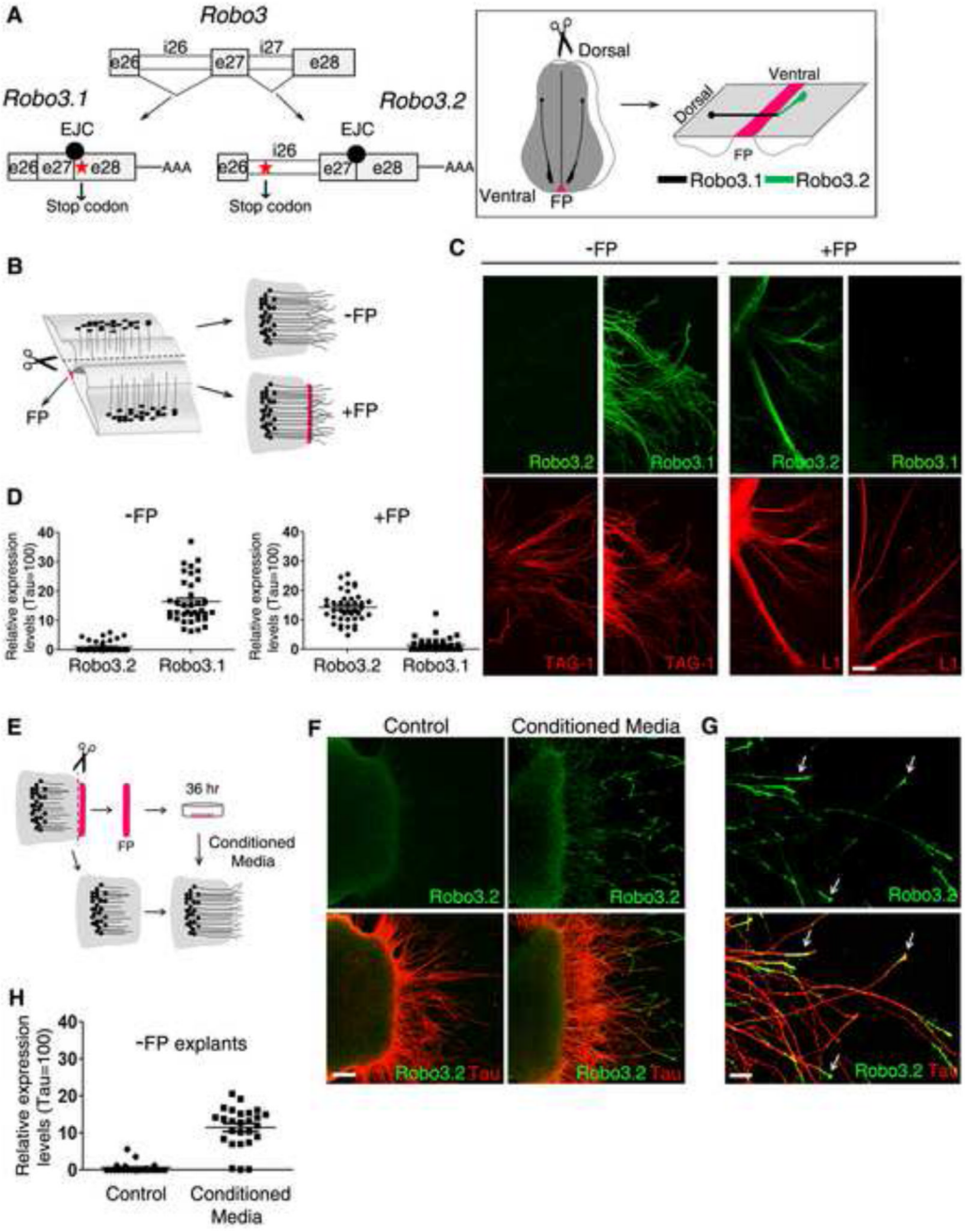

Figure 1. Robo3.2 Protein Levels Are Induced by Floor Plate Signals

A) Schematic representation of the *Robo3.2* transcript and its expression pattern in spinal cord commissural neurons. Robo3.2 protein, green, is detected exclusively in the postcrossing segments of commissural axons.

B) Schematic of the half open book explant system. Half open book explants from E10.5 mouse spinal cords were cultured with (+FP) or without (−FP) the floor plate (indicated in pink).

(C and **D)** Immunostainings of Robo3 isoforms in −FP and +FP explants. Robo3.2 protein is detected only +FP axons (C). Quantification of results in C (D) (Robo3.2 staining, −FP n=41 explants, +FP n=42 explants; Robo3.1 staining, −FP n=37, +FP n=40).
(E-H) Schematic of floor plate-conditioned media (FCM) experiment (E). FCM is sufficient to induce Robo3.2 expression in precrossing axons (F, right panels). High power images depicting prominent Robo3.2 labeling at axonal tips (G, indicated by arrows). Quantification of Robo3.2 levels following treatment with FCM (n=26 explants) indicated a 10-fold increase in Robo3.2 protein levels compared to untreated −FP axons (n=23 explants) (H). Data represented as mean +/− SEM. Scale bar, (C, F) 150 μm; (G) 60 μm. See also Figure S1.

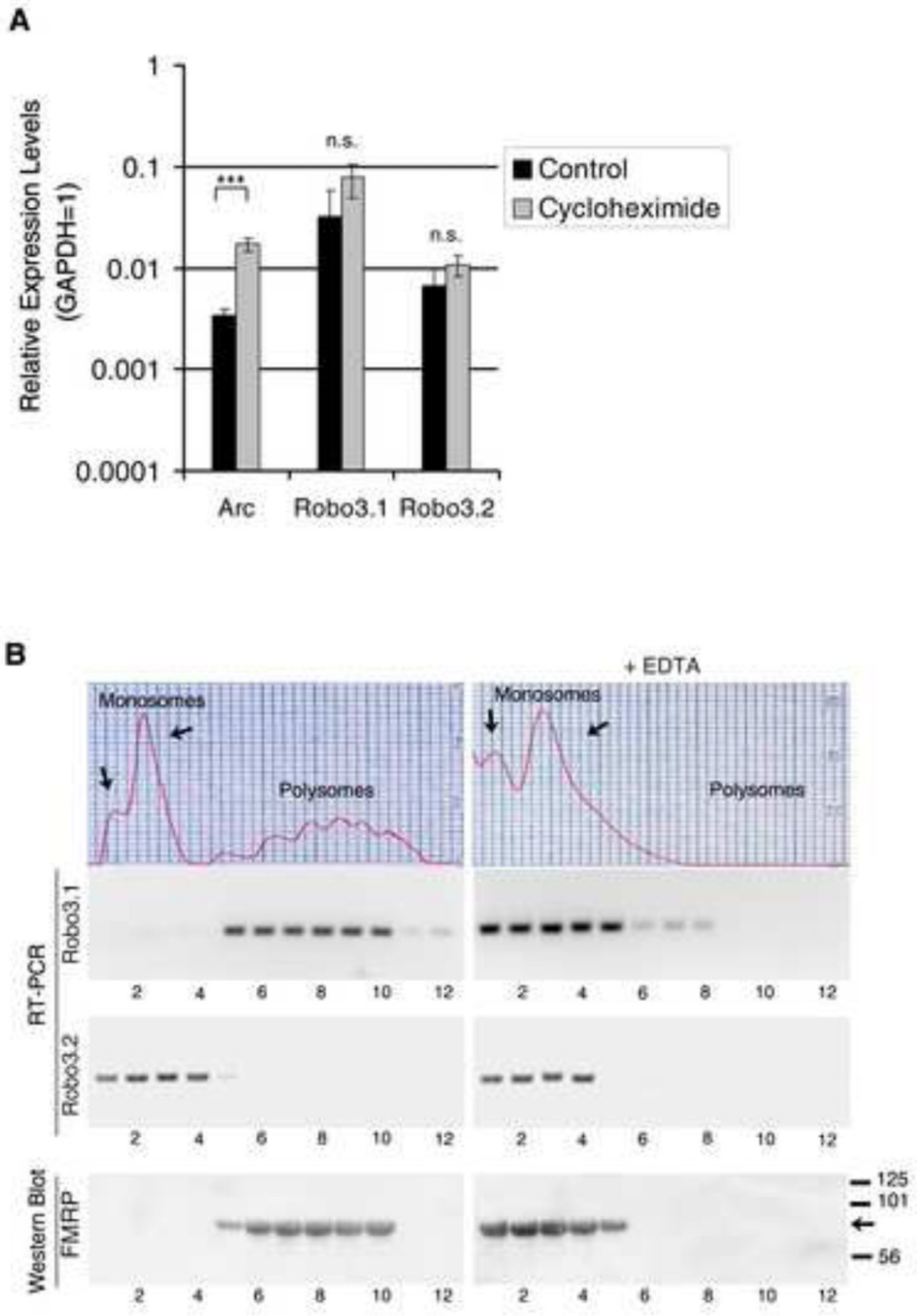

Figure 2. *Robo3.2* mRNA Is Translationally Repressed Prior to Midline Crossing

A) *Robo3.2* is not a target of NMD in precrossing commissural neurons. qRT-PCR did not display a significant change in *Robo3.2* mRNA levels in cycloheximide-treated cells compared to untreated samples. NMD target *Arc* was increased 7-fold upon treatment with cycloheximide for 4 hr. Data are represented as mean +/− SEM, n=3 biological replicates/ condition, ***p < 0.001.

(B) *Robo3.2* is not translated in precrossing neurons. Polysome sedimentation was performed from E10.5 – FP explants. In addition to RNA absorbance profiles, FMRP immunoblotting was used as a marker for polysomes. *Robo3.2* mRNA was detected

primarily in lighter fractions that are not associated with translating ribosomes. EDTA, which results in disruption of polysomes, relocalized FMRP and *Robo3.1* transcripts to the non-translating fractions. The position of these markers is identical to the position of *Robo3.2*, confirming that *Robo3.2* mRNA is in non-translating fractions. See also Figure S2.

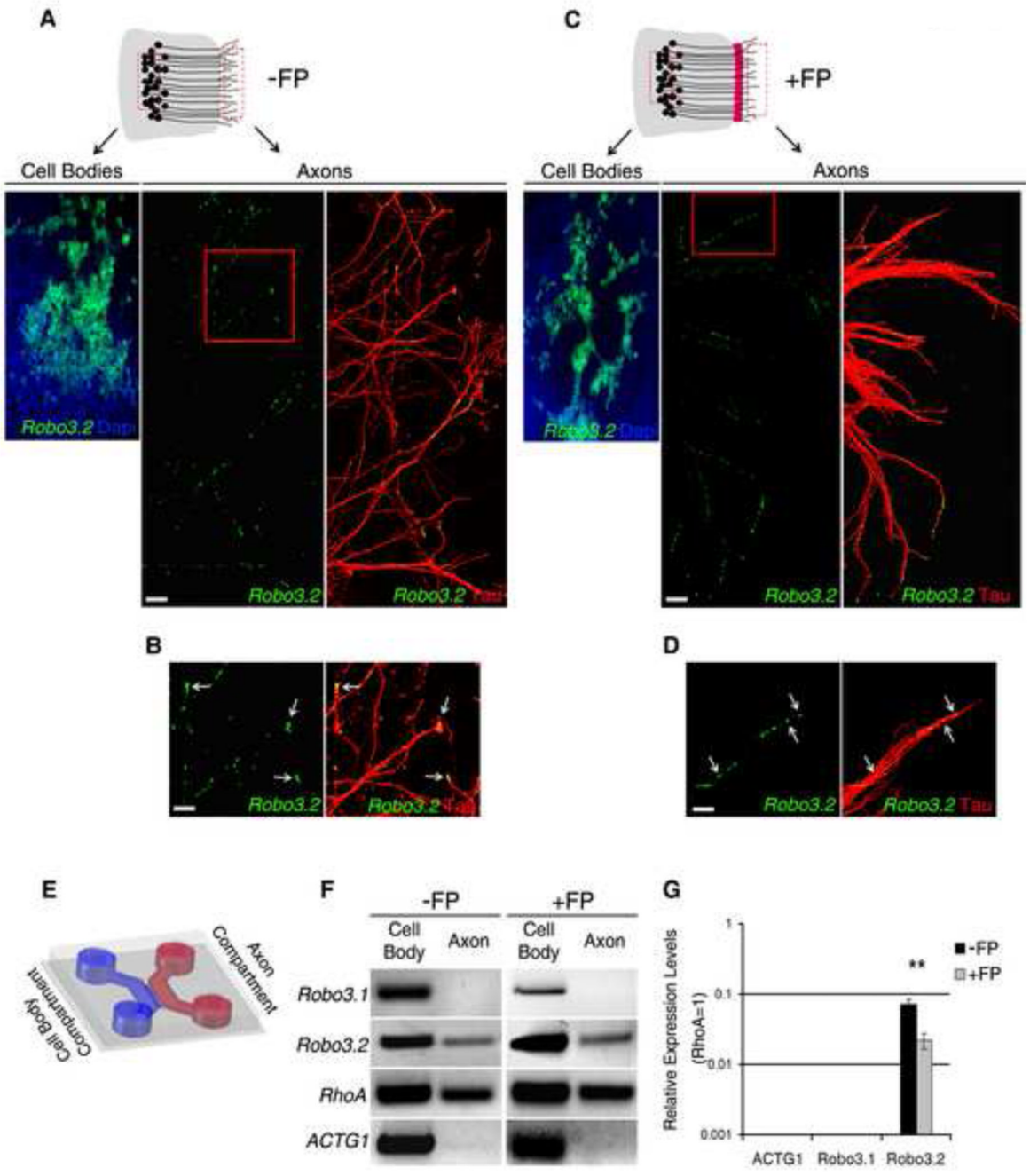

Figure 3. *Robo3.2* mRNA Is Transported into Pre- and Postcrossing Commissural Axons

(A-D) Detection of endogenous *Robo3.2* mRNA in commissural axons by FISH. Antisense riboprobes against *Robo3.2* mRNA resulted in punctuate labeling along axons in both −FP (A, B) and +FP (C, D) explants. Tau (red) immunolabeling was used to visualize axons. High power images show prominent labeling at the distal tips of the axons (B and D, indicated by arrows). Scale bar, (A and C, axons) 150 μm; (A and C, cell bodies) 60 μm; (B and D) 60 μm.

(E) Schematic of a microfluidic chamber that is used to isolate commissural axons from half open book explants. Half open book explants were cultured in the cell body compartment.

The microgrooves in microfluidic devices ensure that no cell bodies enter into axonal compartment.

(F and **G)** Detection of endogenous *Robo3.2* mRNA in purified commissural axons by RT-PCR. *Robo3.2* transcripts were detected in axons of both −FP and +FP explants. *RhoA* mRNA *and gamma-actin* mRNA were used as positive and negative controls, respectively. Quantitative analysis of endogenous *Robo3.2* mRNA in purified −FP and +FP axons (G) (n=3 biological replicates (65 explants/replicate). Consistent with the data in F, *Robo3.2* mRNA is present in pre- and postcrossing axons. **p < 0.01. See also Figure S3.

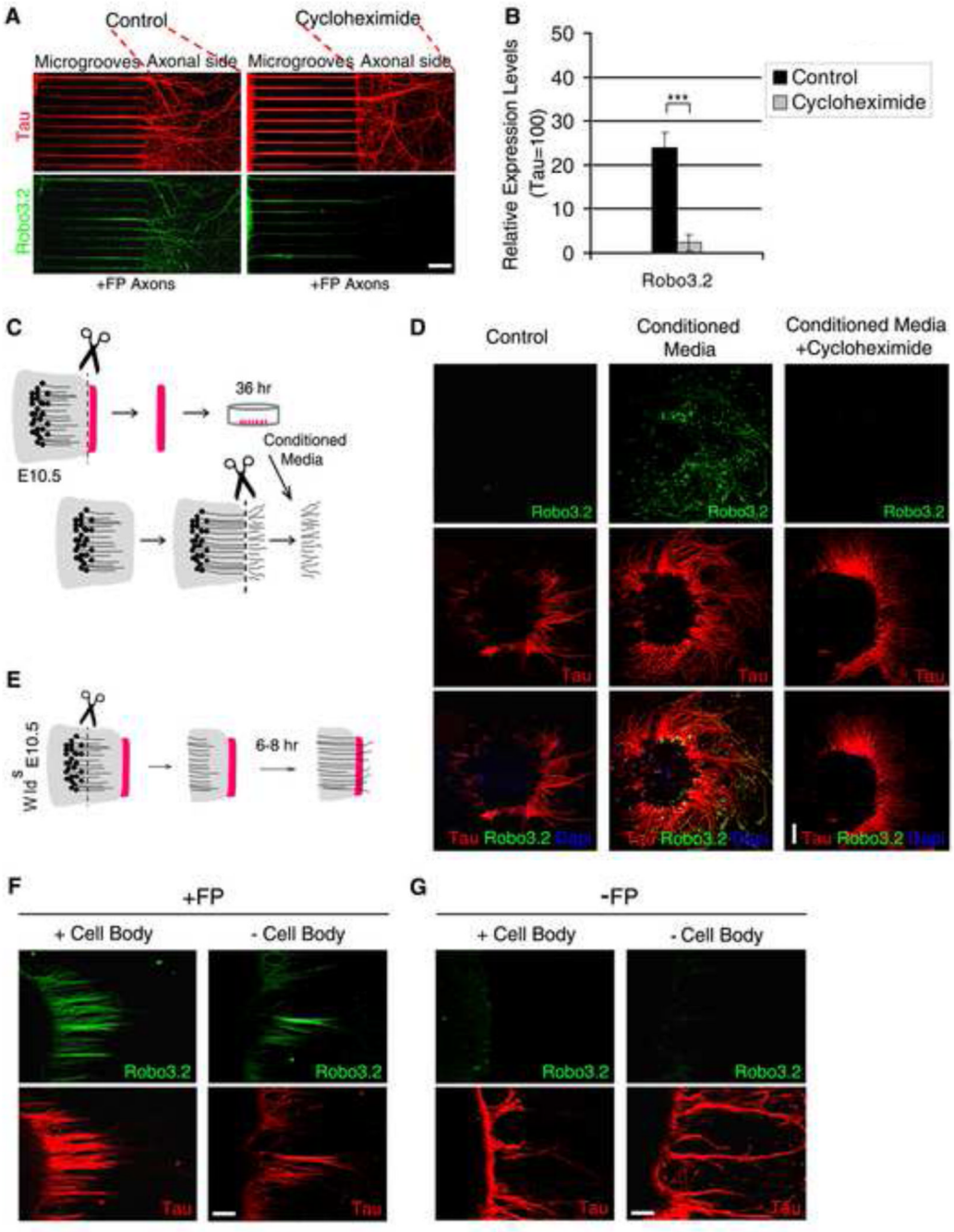

Figure 4. *Robo3.2* Is Locally Translated in Commissural Axons

(A and **B)** *Robo3.2* is locally translated in postcrossing axons. +FP explants were cultured in microfluidic chambers. Axonal treatment of cycloheximide (12 hr, 10 μM) resulted in a more than 90% reduction in Robo3.2 protein levels in postcrossing axons (B) (n=120 axons/condition). Data are represented as mean +/− SEM, ***$p < 0.001$.

(C and **D)** FCM induces local translation of *Robo3.2*. Schematic of the experimental design (C). Application of FCM to severed −FP axons resulted in prominent axonal labeling of Robo3.2 protein (D). This effect was blocked by application of 10 μM cycloheximide, indicating that Robo3.2 induction in axons is translation dependent.

(E-G) *Robo3.2* is locally translated in postcrossing axons in the absence of commissural cell bodies. Schematic representation of the experimental design (E). +FP Axons from Wld^S mice were assayed to monitor Robo3.2 in spinal cord explants in which the cell bodies were transected from the axons before axons reach the midline. Severed axons from Wld^S grew through the floor plate with no degeneration. Severed axons induced Robo3.2 protein after crossing the midline in the absence of cell bodies (F, right panels). Scale bar, (A) 75 μm, (D) 200 μm, (F, G) 60 μm. See also Figure S4.

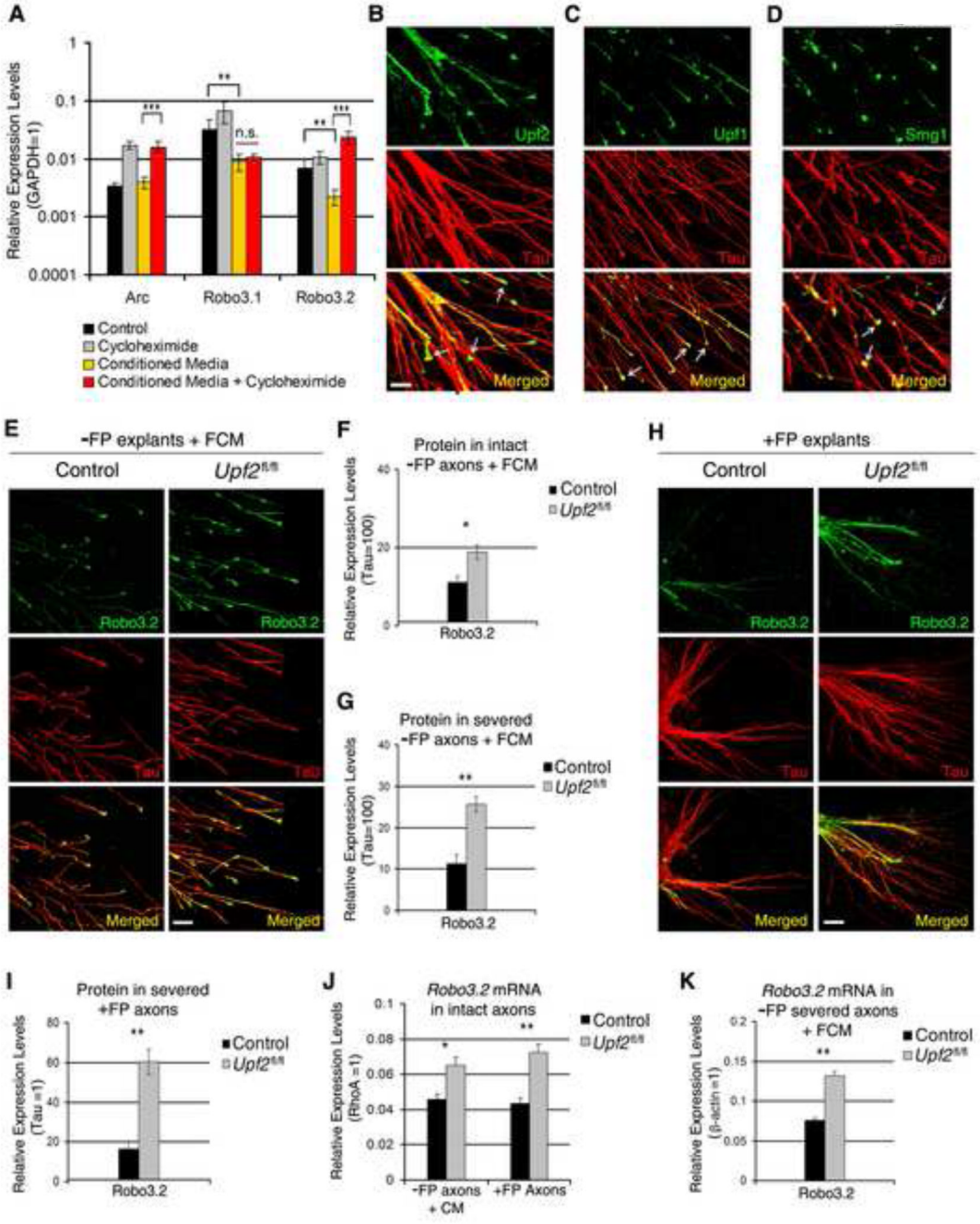

Figure 5. NMD Regulates Robo3.2 Protein Levels in Postcrossing Commissural Axons

(A) *Robo3.2* mRNA becomes a target of NMD following exposure to floor plate-conditioned media. FCM resulted in 70% lower levels of *Robo3.2* mRNA in commissural cell bodies compared to control-treated explants. This reduction was blocked by treatment with 10 μM cycloheximide suggesting that *Robo3.2* degradation upon FCM is NMD-dependent.

(B-D) Upf2 (B) Upf1 (C) and Smg1 (D) are localized to axons, with increased levels at axonal tips.

(E-G) FCM treatment resulted in higher Robo3.2 levels in −FP axons from *Upf2* cKO compared to −FP axons from control (E). Quantifications of results in E (F) (110 axons per

control (n=3) and mutant (n=4) embryos). Quantification of Robo3.2 protein in severed axons following treatment with FCM (G) (460 control axons (n=11 explants, 4 embryos) and 410 *Upf2* cKO axons (n=10 explants, 3 embryos)). (See also Figures S6A and S6B).
(H and **I)** Robo3.2 immunostaining in +FP axons from control and *Upf2* cKO (H). Robo3.2 is 3.5-fold higher in postcrossing axons of *Upf2* cKO compared to control axons (I) (211 axons, control (n=11 axonal areas, 4 embryos) and 217 axons, mutant (n=13 axonal areas, 5 embryos) embryos).
(J and **K)** Quantification of *Robo3.2* mRNA by qRT-PCR in isolated unsevered (J) and severed (K) axons following induction of *Robo3.2* translation by FCM. Axons were harvested from control and *Upf2* cKO explants that were cultured in microfluidic chambers. Both *Upf2* cKO −FP axons that were treated with FCM or *Upf2* cKO +FP axons that encountered the floor plate have higher levels of *Robo3.2* mRNA compared to control axons (J) (*Upf2* cKO −FP axons (n=38 explants, 5 embryos), control −FP axons (n=30 explants, 4 embryos); *Upf2* cKO +FP axons (n=41 explants, 5 embryos), control +FP axons (n=35 explants, 4 embryos). qRT-PCR for *Robo3.2* mRNA in isolated −FP severed axons following FCM treatment (K) (74 control (n=3 embryos) and 77 *Upf2* cKO (n=3 embryos) explants. Data are represented as mean +/− SEM, *p < 0.05, **p < 0.01 and ***p < 0.001 Scale bar, (B-D) 75 μm, (E, H) 100 μm. See also Figures S5 and S6.

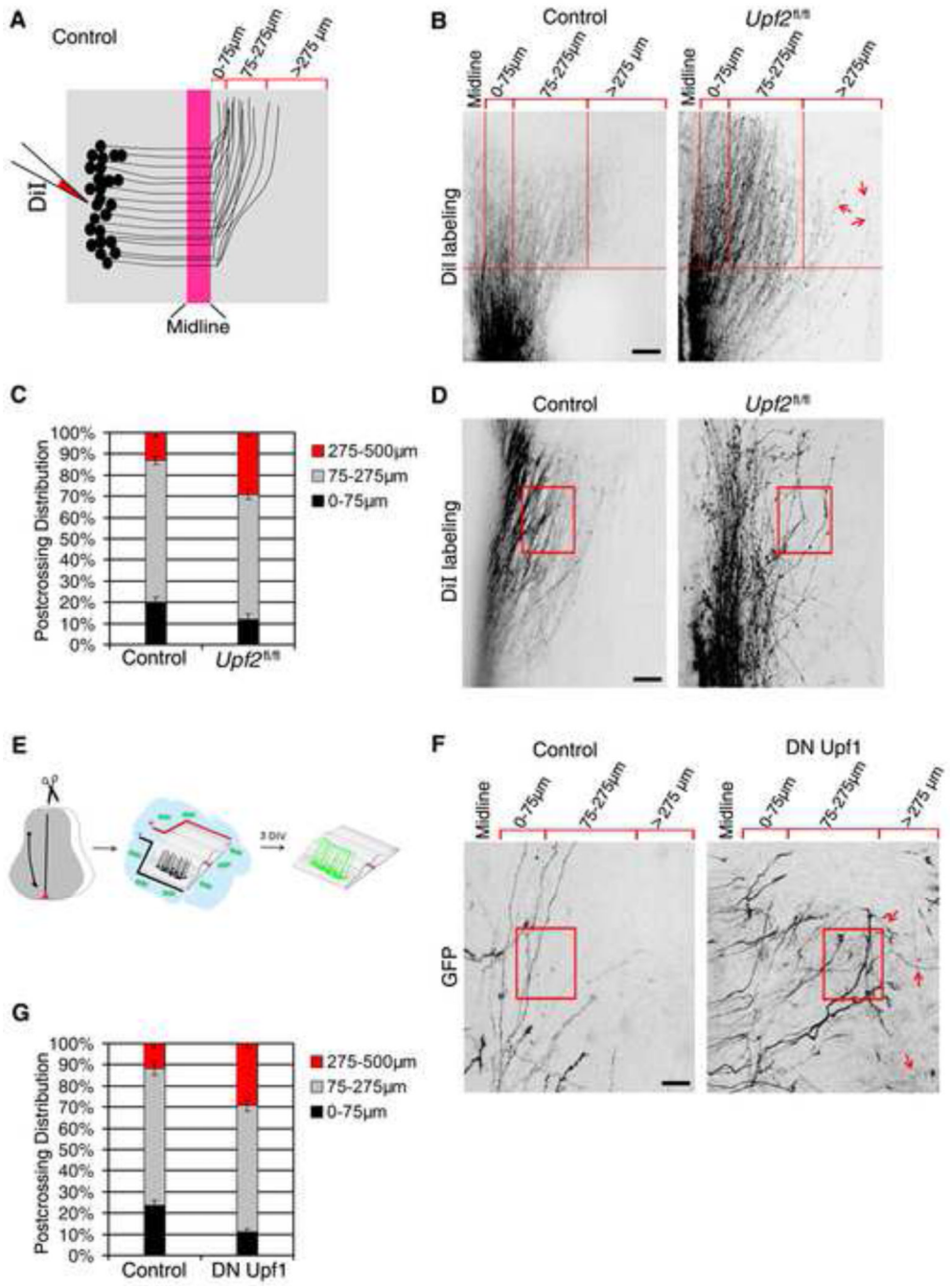

Figure 6. NMD Regulates Postcrossing Axon Behavior

(A) Schematic of precrossing and postcrossing axon behavior. Axons were visualized by DiI at E13.5. Postcrossing axons were binned into three categories based on their distance from midline: 0-75 μm, 75-275 μm, and >275 μm.

(B-D) *Upf2* cKO axons exhibited normal precrossing behavior, but more lateral postcrossing trajectories than control axons (B). Many more *Upf2* cKO axons are seen >275 μm from the midline compared to control axons (C) (459 axons, control (n=5) and 559 axons, *Upf2* cKO (n=6) embryos). Boxed areas indicate examples of organized (control panel) or altered (mutant panel) trajectories (D).

(E-G) Schematic of electroporation in spinal cord open book cultures (E). Electroporation of dominant-negative Upf1 in commissural neurons resulted in aberrant guidance similar to *Upf2* cKO axons (F). Lateral distributions of postcrossing axons following dominant-negative Upf1 electroporation (G) (153 axons, control (n=4) and 131 axons, *Upf2* cKO (n=3) embryos). Data are represented as mean +/− SEM. Scale bar, 200 μm (B), 75 μm (D, F).

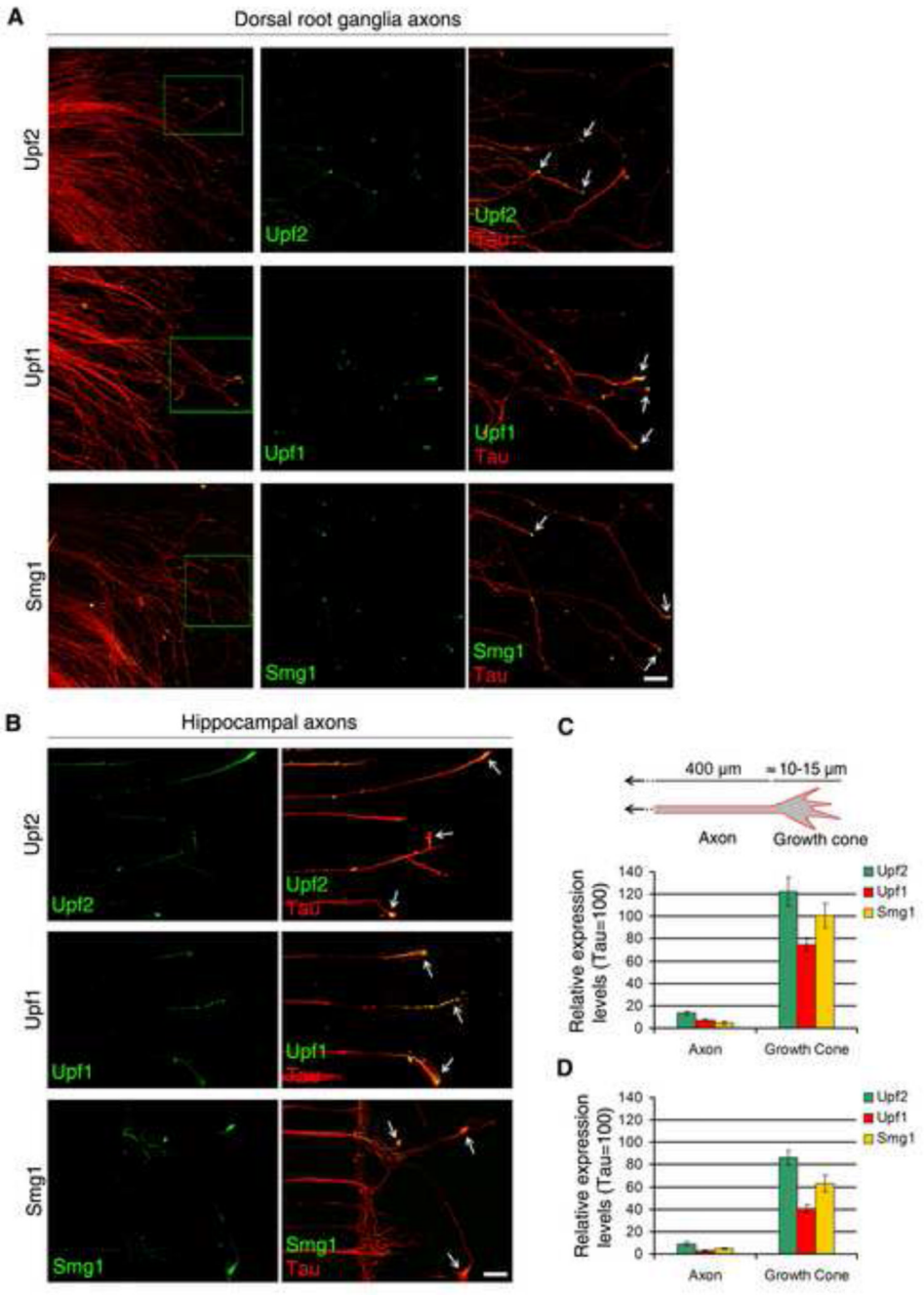

Figure 7. NMD Machinery Is Localized to Growth Cones of Several Types of Neurons

(**A** -**D**) Upf2, Upf1 and Smg1 localize to axons and growth cones of peripheral (**A**) and central (**B**) nervous system neurons. Quantifications of the fluorescent intensities of NMD proteins in individual axons of dorsal root ganglia (C) and hippocampal (D) neurons. Data are represented as mean +/− SEM. Scale bar, 100 μm (A), 30 μm (B).